AD-A263 568

MENTATION PAGE

Form Approved
OMB No. 0704-0188

1. AGENCY USE ONLY (Leave blank)	2. REPORT DATE	3. REPORT TYPE AND DATES COVERED
	April 15, 1993	Reprint

4. TITLE AND SUBTITLE
The Aurora at Quiet Magnetospheric Conditions: Repeatability and Dipole Tilt Angle Dependence

5. FUNDING NUMBERS
PE 62101F
PR 4643
TA 11
WU 01

6. AUTHOR(S)
I. Oznovich*, R.W. Eastes, R.E. Huffman, M. Tur*, I. Glaser*

7. PERFORMING ORGANIZATION NAME(S) AND ADDRESS(ES)
Phillips Lab/GPIM
29 Randolph Road
Hanscom AFB, MA 01731-3010

8. PERFORMING ORGANIZATION REPORT NUMBER
PL-TR-93-2094

9. SPONSORING/MONITORING AGENCY NAME(S) AND ADDRESS(ES)

10. SPONSORING/MONITORING AGENCY REPORT NUMBER

11. SUPPLEMENTARY NOTES *Faculty of Engineering, Tel Aviv University, Tel Aviv Israel
Reprinted from Journal of Geophysical Research, Vol. 98, No. A3, pages 3789-3797, March 1, 1993

12a. DISTRIBUTION/AVAILABILITY STATEMENT
Approved for public release; Distribution unlimited

12b. DISTRIBUTION CODE

13. ABSTRACT *(Maximum 200 words)*

Is there a magnetospheric ground state? Do the position and size of the auroral oval depend on the magnetic dipole tilt angle at quiet magnetospheric conditions? In order to address these questions, northern hemisphere images of the aurora at 1356 Å, obtained by Polar BEAR at solar minimum (beginning of 1987), were related to high temporal resolution IMP 8 measurements of the interplanetary magnetic field, to solar wind velocity, and to the ground-based activity index Kp. The first problem was addressed by a two-dimensional correlation study of the repeatability of auroral emissions in corrected geomagnetic space at conditions of minimum energy transfer from the magnetosphere. The correlation measure of auroral images was 0.6–0.85. Error simulations indicate that given the uncertainties in pixel position and intensity, the maximum expected value of the correlation measure is 0.65–0.9. The notion of a ground state magnetosphere is therefore supported by our data. Repeatability was found at the same level regardless of time or reconfigurations of the magnetosphere between images and independent of magnetic time sector. The second problem was addressed by relating latitudinal shifts of the aurora with dipole tilt angle without resorting to auroral boundary specification. Our data indicate that the latitude of the continuous aurora is related to the dipole tilt angle at quiet magnetospheric conditions. In the winter hemisphere a 10° increase in the dipole tilt angle causes a 1° decrease (increase) in the latitude of auroral emissions at noon (midnight). The magnetic local time distribution of the latitudinal shifts with dipole tilt angle support a simple model in which the dipole tilt angle determines the position of the center of the auroral circle along the magnetic meridian 1320–0120 MLT (for IMF B_y positive) and does not affect its radius.

14. SUBJECT TERMS
Ultraviolet, Aurora, Magnetosphere, Dipole tilt, Image, Auroral oval, Satellite

15. NUMBER OF PAGES
9

16. PRICE CODE

17. SECURITY CLASSIFICATION OF REPORT	18. SECURITY CLASSIFICATION OF THIS PAGE	19. SECURITY CLASSIFICATION OF ABSTRACT	20. LIMITATION OF ABSTRACT
UNCLASSIFIED	UNCLASSIFIED	UNCLASSIFIED	SAR

JOURNAL OF GEOPHYSICAL RESEARCH, VOL. 98, NO. A3, PAGES 3789–3797, MARCH 1, 1993

The Aurora at Quiet Magnetospheric Conditions: Repeatability and Dipole Tilt Angle Dependence

I. OZNOVICH[1]

Faculty of Engineering, Tel Aviv University, Tel Aviv, Israel

R. W. EASTES AND R. E. HUFFMAN

Phillips Laboratory, Geophysics Directorate, Hanscom Air Force Base, Massachusetts

M. TUR AND I. GLASER

Faculty of Engineering, Tel Aviv University, Tel Aviv, Israel

Is there a magnetospheric ground state? Do the position and size of the auroral oval depend on the magnetic dipole tilt angle at quiet magnetospheric conditions? In order to address these questions, northern hemisphere images of the aurora at 1356 Å, obtained by Polar BEAR at solar minimum (beginning of 1987), were related to high temporal resolution IMP 8 measurements of the interplanetary magnetic field, to solar wind velocity, and to the ground-based activity index *Kp*. The first problem was addressed by a two-dimensional correlation study of the repeatability of auroral emissions in corrected geomagnetic space at conditions of minimum energy transfer from the magnetosphere. The correlation measure of auroral images was 0.6–0.85. Error simulations indicate that given the uncertainties in pixel position and intensity, the maximum expected value of the correlation measure is 0.65–0.9. The notion of a ground state magnetosphere is therefore supported by our data. Repeatability was found at the same level regardless of time or reconfigurations of the magnetosphere between images and independent of magnetic time sector. The second problem was addressed by relating latitudinal shifts of the aurora with dipole tilt angle without resorting to auroral boundary specification. Our data indicate that the latitude of the continuous aurora is related to the dipole tilt angle at quiet magnetospheric conditions. In the winter hemisphere a 10° increase in the dipole tilt angle causes a 1° decrease (increase) in the latitude of auroral emissions at noon (midnight). The magnetic local time distribution of the latitudinal shifts with dipole tilt angle support a simple model in which the dipole tilt angle determines the position of the center of the auroral circle along the magnetic meridian 1320–0120 MLT (for IMF B_y positive) and does not affect its radius.

INTRODUCTION

The quiet state of the magnetosphere has attracted much attention in the past decade. This is due to the realization that an understanding of the quiet magnetosphere can help determine conditions for magnetospheric stability, guide us in understanding magnetotail formation, test magnetospheric models, and explicate energetically secondary processes [*Gussenhoven*, 1988]. The terms baseline and ground state were applied interchangeably to the magnetosphere at periods of low solar wind velocity, small amplitude of the interplanetary magnetic field (IMF), and low *Kp*. Could the state of the magnetosphere be rightly called ground state at these conditions?

Minimum energy content is a prerequisite of a ground state magnetosphere. It is assumed that the ground state of the magnetosphere occurs when the solar wind energy coupling is minimized and previous energy input processes have decayed. We can use measured indicators of magnetospheric activity to identify the quiet state of the magnetosphere and study its structure. Indeed, previous studies identified necessary conditions for the quiet magnetosphere and showed that these conditions were regularly met [*Gussenhoven*, 1988; *Kerns and Gussenhoven*, 1990].

Here we take the opposite approach. Times satisfying the IMF, solar wind, and *Kp* conditions for the quiet magnetosphere are located. We ask if the magnetosphere is the same at such times. The auroral oval is one of the most pronounced manifestations of the solar wind–magnetosphere–ionosphere interaction. In order to quantify our study we pose the following question: To what extent is the quiet magnetosphere repeatable, as manifested by the brightness and position of the auroral oval?

An answer to this question may help to define the state of the magnetosphere at periods of minimum energy transfer from the solar wind. If the auroral oval is the same at quiet magnetospheric conditions, the concept of a ground state wins observational credence. A magnetosphere that does not repeat itself gives credence to the notion of an inherently unstable system.

Evidence testifying on the effect of the dipole tilt angle on various observables of the magnetosphere dates back to the 1960s, but recent interest in the subject aroused due to its relevance to ionospheric observations and magnetic field models. The observables were the latitude of soft particle precipitation associated with the cusp and cleft [*Maehlum*,

[1]Now at Institute of Space and Atmospheric Studies, University of Saskatchewan, Saskatoon, Canada.

Paper number 92JA01950.
0148-0227/93/92JA-01950$05.00

1968; *Burch*, 1972; *Newell and Meng*, 1989] and polar cap electric fields [*de la Beaujardière et al.*, 1991; *Wu et al.*, 1991]. *Burch* [1972] found that the low-latitude boundary of polar-cusp electron precipitation shifts by −3° and +1° in the winter and summer, respectively, relative to its equinox location. *Newell and Meng* [1989] detected the same dependence (in direction and annual magnitude) of cusp latitude on dipole tilt angle, but it was symmetric about equinox. *de la Beaujardière et al.* [1991] found that the large-scale convection pattern above the north pole was shifted toward the nightside in summer as compared to winter. They attributed the 5° shift antisunward of the dawn-to-dusk electric potential to variation of the dipole tilt angle. *Wu et al.* [1991] studied the substorm westward electrojet in the nightside polar cap. They showed that it flowed at ~4° higher in latitude in the winter hemisphere than in the summer hemisphere near local midnight. This latitude difference reversed for local times prior to 2000 MLT. *Meng* [1979] studied a diurnal variation in the CGL at which Defense Meteorologist Satellite Program (DMSP) encountered the equatorward boundary of the quiet time auroral oval. *Gussenhoven et al.* [1980] disputed this variation by noting that the diurnal variation of the satellite trajectory was not accounted for.

Magnetospheric field models indeed predict a dipole tilt angle dependence of the boundary of the last closed field line. *Voigt* [1974] calculated that the geomagnetic latitude of the last closed field line at local noon and midnight shifts in the winter relative to the summer hemisphere by −3° and +4°, respectively. *Stern* [1985] computed the latitude of the dipole cusp at the surface of Earth. He found that it is located ~2° equatorward at equinox relative to the summer and approximately another 1° equatorward in the winter relative to equinox.

This study is the first to investigate dipole tilt angle effects on global auroral emissions within the corrected geomagnetic coordinate system. Global auroral images allow one to look at many (and sometimes all) magnetic local times, thereby allowing inference of global magnetospheric effects. The technique employed allows us to discern latitudinal shifts of auroral emissions without resorting to auroral boundary specification, thereby making the study almost independent of the sensitivity of the detector. The detection threshold dependence remains hidden in the spatial coverage and magnetospheric origin of the detected auroral signal. This study contrasts to earlier studies wherein poleward or equatorward boundaries of the auroral oval were determined and used for boundary motion analysis.

The major factor that determines auroral arc position is the southward component of the IMF [e.g., *Burch*, 1972; *Holzworth and Meng*, 1975]. Therefore it is at the pristine IMF conditions detailed below that one has a chance of identifying the minor effects of the dipole tilt angle (DTA). The dipole tilt angle is the angle between the direction of the sun and the direction of the north magnetic dipole pole (relative to the center of Earth). The dipole tilt angle is sometimes quoted by the magnetic latitude of the subsolar point. Here we pose the question: Is there a dependence of auroral emissions, in terms of position and auroral oval size, on the magnetic dipole tilt angle at quiet magnetospheric conditions?

The following section discusses image selection by magnetospheric and ground magnetic criteria. The major part of the data reduction and analysis is devoted to correlating pairs of auroral images in corrected geomagnetic space. Next, results concerning the repeatability of auroral emissions and latitudinal shifts of the aurora with dipole tilt angle are described. We discuss the results in the frame of an error analysis, aimed to determine the uncertainties inherent in image acquisition and processing. It is shown that a simple model of the aurora can satisfactorily explain the DTA dependence of our data.

Data Selection and Analysis

The data used consisted of three parts: (1) 407 1356-Å images of the aurora borealis obtained by Polar BEAR at solar minimum, (2) concurrent IMP 8 measurements of the IMF and solar wind velocity, and (3) the ground-based activity index *Kp*. Interplanetary data and *Kp* values were obtained from the National Space Science Data Center data base [*Couzens and King*, 1989]. IMF data are in geocentric solar magnetospheric (GSM) coordinates. The origin of the GSM coordinate system is at the center of Earth. Its coordinates are X, Y, and Z. The positive X axis is directed toward the Sun. The Z axis lies in the plane containing both the X axis and the geomagnetic dipole axis and is perpendicular to the X axis. The Y axis complements a right-handed Cartesian system.

Temporal resolution of the three data sets is as follows:

1. A Polar BEAR image was acquired in ~11 min for every pass above the north pole region; Minimum temporal separation between images was approximately the 110-min orbital period; Maximum temporal separation between images was 42 days; all the data used were from January and February 1987.
2. IMF measurements with a temporal resolution of 15 s were used; solar wind velocity measurements were 1–2 min apart.
3. The ground-based *Kp* index is a global 3-hour average parameter.

Technical characteristics of the spacecraft (Polar BEAR), imager (Atmospheric Ionospheric Remote Sensor, AIRS), and detectors were previously described by *Schenkel et al.* [1986] and *DelGreco et al.* [1988]. The primary features that contribute to the 1356-Å band of AIRS are the O I doublet at 1356 Å and 1359 Å and N_2 Lyman-Birge-Hopfield (LBH) at 1354 Å. The relative contribution of the two species to the measured intensity depends on the characteristic energy of the precipitating electrons and the look direction. The images exhibit few discrete arcs and these are generally weak, because images were chosen specifically for quiet magnetospheric conditions. Therefore the following discussion pertains primarily to the continuous auroral oval.

Polar BEAR images of the aurora were highly suitable for studying correlations between images and latitudinal shifts of auroral emissions. There were three major advantages of AIRS over previous imaging instruments in that respect: (1) a relatively low detection threshold (61 R per count relative to the ~300 R/count threshold of the Dynamics Explorer 1 photometer [*Hoffman et al.*, 1988]), which is crucial for a reasonable signal from the weak emissions of the quiescent aurora (typically less than 1.5 kR at far-ultraviolet wavelengths), (2) high spatial resolution (~20 km at nadir) due to the combination of a low-altitude orbit and small instantaneous field of view, and (3) images obtained with constant ground resolutions and approximately fixed in their ground

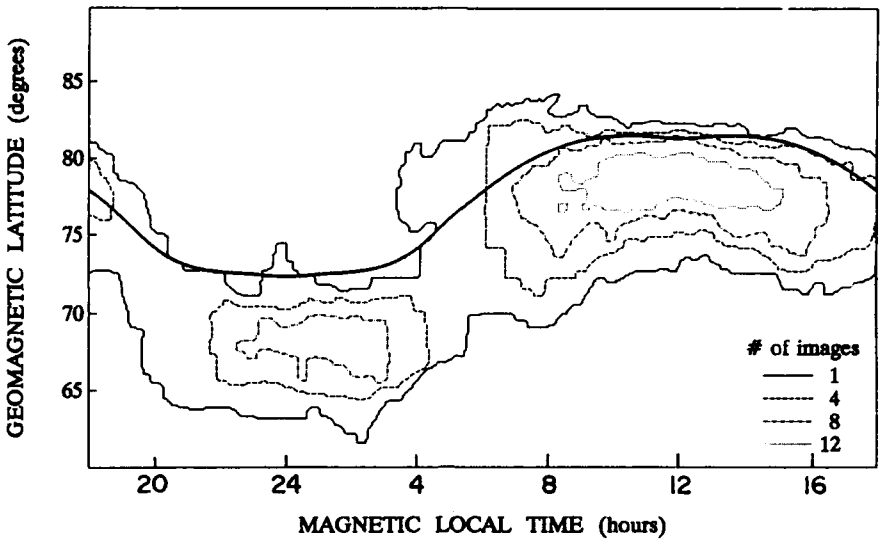

Fig. 1. Number distribution of the 30 quiet time auroral images of our data base in corrected geomagnetic coordinates. Detection threshold is 61 R at 1356 Å for nadir viewing. The bold solid line is the location of the last closed field line boundary for the untilted Earth's dipole (adopted from *Voigt* [1974]).

dimensions due to the circular orbit of the satellite, thus enabling coherent multiple image analysis.

The images were processed with the algorithms developed by I. Oznovich et al. (submitted manuscript, 1991). The aurora was mapped to a Mercator projection of the corrected geomagnetic latitude (CGL)—magnetic local time (MLT) coordinate system, as in Figure 1. The brightness of the aurora was normalized to nadir assuming an incident Maxwellian auroral electron spectrum with an average energy of 0.5 keV for dayside arcs and 1.5 keV for nightside arcs. The average energies were derived from the appropriate CGL-MLT cells of the Kp = 0–1 maps of *Hardy et al.* [1985]. The background of dayglow radiation was subtracted. The mapping was limited to scan angles within 55° of satellite nadir. Simulation runs show that the average (maximum) latitudinal uncertainty of the geometric mapping of the image is 0.5° (1°) for scan angles below 55° I. Oznovich et al. (submitted manuscript, 1991).

Kerns and Gussenhoven [1990] showed that the percentage of occurrence of $B > 10$ nT and $V > 500$ km s^{-1} drops to zero at persistently quiet magnetospheric conditions (see Kerns and Gussenhoven's Figure 3). Thus the quiet magnetosphere was defined using the following parameters: $Kp < 2$, $B_z \geq -4$ nT, $B \leq 10$ nT, and $V < 500$ km s^{-1}. We required these conditions be maintained at least 2 hours prior to image acquisition time. Also even at the above conditions, one may observe high-latitude arcs which are not part of the oval. All the images chosen by the above criteria were evaluated for indication of such arcs. The few MLT sectors (8 of 138) that showed high-latitude arcs were removed from the data base. Of the 407 auroral images in our data base, 151 had concurrent interplanetary measurements. Of these, 30 images at 1356 Å were selected by the above criteria. All the selected images were obtained at $B \leq 8$ nT, $|B_z| \leq 4$ nT, $B_x \leq 0$ nT, and $B_y \geq 0$ nT conditions for 2–6 hours prior to image acquisition time. This B_x-B_y configuration is the so-called IMF garden hose away configuration.

The least stringent criterion was $Kp <$ [illegible]. In fact, no images were added to the chosen 30 when this criterion was removed. The most stringent criterion pertained to using the high temporal resolution (15 s) IMF data. Data selection using hourly average IMF data resulted in situations where the hourly average was within the desired range, satisfying the criteria, yet the high-resolution IMF data showed significant variations outside the desired range which were cancelled in the hourly averages.

The number distribution of the 30 selected images is presented by Figure 1 in CGL-MLT space. Detection threshold (one count) applies to auroral intensities above 61 R for nadir viewing. Global coverage of the auroral oval is never obtained by a single image. Most of the data cover local times near noon (0600–1600 MLT) and midnight (2200–0400 MLT). Only a few images view the dawn and dusk sectors. The bold solid line in Figure 1 denotes the location of the last closed field line boundary for the untilted Earth's dipole (adopted from *Voigt* [1974]). Note that almost all the emissions observed are due to particles precipitating on closed field lines, most likely of plasma sheet origin.

The two problems presented in the introduction are addressed by relating pairs of auroral images corresponding to the quiet magnetosphere. The analysis is quantified by calculating a correlation image for each pair and searching for its maxima. The value of the maxima is the correlation between that pair of images. The position of the maxima is used to discern latitudinal and longitudinal shifts of the aurora.

The correlation image $R_{I,J}$ of images I and J, both of size $N \times M$, is given by

$$R_{I,J}(\Delta k, \Delta l) = \frac{\sum_{k=1}^{N}\sum_{l=1}^{M} I(k, l)J(k-\Delta k, l-\Delta l)}{\left[\sum_{k=1}^{N}\sum_{l=1}^{M} I^2(k, l) \sum_{k=1}^{N}\sum_{l=1}^{M} J^2(k, l)\right]^{1/2}} \quad (1)$$

where k and l are column and line number, respectively. Δk is the shift in column, and Δl is the shift in line. The numerator is the cross correlation between image I and image J. The denominator is simply the square root of the power P of the two images. The power P_I of image I (and similarly of image J) is given by $P_I = \sum_{k=1}^{N} \sum_{l=1}^{M} I^2(k, l)$. The Cauchy-Schwartz inequality states that $0 \leq R_{I,J}(\Delta k, \Delta l) \leq 1$. R is exactly unity if the two images are perfectly correlated. $R \geq 0$ because image intensities are nonnegative. Hence the two-dimensional correlation image is analogous to the linear coefficient of correlation. In digital image processing, the correlation image is usually used to find an image function that matches a template [*Levine*, 1985].

The correlation image may be computed relatively quickly by using the correlation theorem

$$R_{I,J} = \frac{\mathcal{F}^{-1}\{\mathcal{F}(I)\mathcal{F}^*(J)\}}{(P_I P_J)^{1/2}} \tag{2}$$

where $\mathcal{F}(I)$ is the Fourier transform of image I, $\mathcal{F}^*(J)$ is the complex conjugate of the Fourier transform of image J, and $\mathcal{F}^{-1}$ is an inverse Fourier transform. The use of the Fourier domain necessarily implies wrap around, a problem that is solved by zero padding. The correlation measure r of the two images I and J is given by

$$r_{I,J} = \max \{R_{I,J}(\Delta k, \Delta l)\} \tag{3}$$

The correlation measure r was used to study the repeatability of auroral emissions at quiet magnetospheric conditions. The shift in column and shift in line which give that maxima are Δk_m and Δl_m, respectively.

The Mercator projection of the CGL-MLT coordinate system allows one to relate Δl_m directly to changes in magnetic latitude and Δk_m to changes in magnetic local time. This relation was used to investigate the possible dependence of aurora position on DTA. Our data span a DTA range of 85°–120°, due to both diurnal and seasonal changes of the dipole tilt angle. This range comprises approximately half of the annual range of DTA. The significance of the above technique for auroral studies is that it accounts for correlations in corrected geomagnetic space both in brightness and position of the aurora without resorting to boundary specification.

In principle, given a set of n images, there are $n(n-1)/2$ distinct pairs of images. In reality, we had fewer pairs, because the overlap in the field of view of the two images is zero for some pairs. The MLT range of 0000–2400 was divided to 12 sectors, each 2 hours wide. Computations of the correlation measure were performed on each of the available sectors separately. In Figure 2, for example, useful MLT sectors for correlation analysis were 1000 (0900–1100), 1200 (1100–1300), and 1400 (1300–1500). Δk_m that corresponds to a large change in MLT was unexpected, since relatively narrow MLT sectors were used in the analysis. Indeed, all the maxima found were located at ΔMLT < 1/2 hour.

The 30 images selected by the above criteria represent 13 different configurations of the quiet magnetosphere. A reconfiguration of the magnetosphere was assumed when one or more of the above IMF, solar wind, or ground activity values did not meet the quiet state criteria during the time interval between one image acquisition time and its pair.

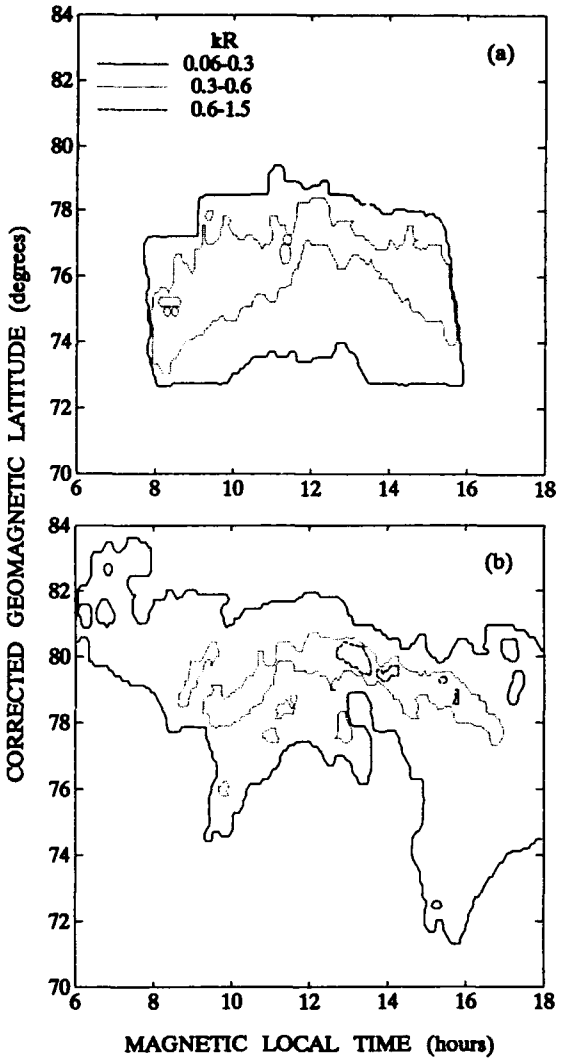

Fig. 2. (*a*) An auroral image obtained on February 5, 1987, 0636 UT and (*b*) one obtained on January 24, 1987, 1442 UT. Contour lines denote 1356 Å auroral emissions above 60 R (solid line), 300 R (dotted line), and 600 R (dashed line). The correlation measures of this image pair were 0.8, 0.78, and 0.67 for MLT sectors 1000, 1200, and 1400, respectively. The top image (DTA 118°) is shifted to lower magnetic latitudes by 3°, 2.6°, and 3° relative to the bottom image (DTA 101°) at 1000, 1200, and 1400 MLT, respectively.

RESULTS

Our case study includes an auroral image obtained on February 5, 1987, 0636 UT (Figure 2*a*), and an auroral image obtained on January 24, 1987, 1442 UT (Figure 2*b*). Contour lines in Figure 2 denote auroral emissions above 60 R (solid line), 300 R (dotted line), and 600 R (dashed line). Detection threshold (1 count) at nadir is 61 R, and maximum intensity of the images shown in Figure 2 is ~1.5 kR. The correlation measures of this image pair were 0.8, 0.78, and 0.67 for MLT sectors 1000, 1200, and 1400, respectively.

The statistical analysis included 431 calculations of the correlation measure of all MLT sectors, with the exception of 2000 (1900–2100) MLT. Figure 3 presents the distribution of correlation measures as a function of MLT sector. Values of the correlation measure range between 0.6 and 0.85. Individual points of Figure 3 are distinguished to represent pairs of images

which belong to the same magnetospheric configuration (crosses) and to different magnetospheric configuration (circles).

Note that the scatter in correlation measure values in Figure 3 is independent of whether the image pair belonged to the same or to different magnetospheric configurations. This implies that given the above quiet state criteria, "snapshots" of the aurora are likely to resemble each other at the same level regardless of a possible reconfiguration of the magnetosphere occurring between the snapshots. Note also that the correlation measure in Figure 3 is independent of MLT. This implies that given the above quiet state criteria, auroral emissions are likely to be constant to the same level regardless of the GSM θ coordinate, where $\theta = \arctan(X/Y)$. With regard to the question of repeatability of the aurora, the data in Figure 3 indeed show the aurora to be correlated at such times but at a low level. The average correlation measure obtained was 0.74 ± 0.05.

The case study (Figure 2) includes a dayside auroral arc with a dipole tilt angle of 118° (Figure 2*a*) and a dayside auroral arc with a dipole tilt angle of 101° (Figure 2*b*). The top image (DTA 118°) is shifted to lower magnetic latitudes by 3°, 2.6°, and 3° relative to the bottom image (DTA 101°) at MLT sectors 1000, 1200, and 1400, respectively. The direction of the shift is such that as the dipole tilt angle increases, the dayside aurora moves to lower latitudes.

Changes in latitude as a function of changes in dipole tilt angle are shown in Figure 4; 207 points contributed to the dayside analysis (top figure) and 40 points to the nightside analysis (bottom figure). In order to collect a large number of measurements, the dayside plot includes three MLT sectors (1200, 1400, and 1600), as does the nightside plot (2200, 0000, and 0200).

The straight lines were derived from a least chi-square fit to the data. The fitted lines exhibit close to zero offsets; that is, a zero change in DTA causes no shift in CGL, as one might expect. The scatter in the data is of the order of 1°. The two variables, change in latitude (ΔCGL) and change in dipole tilt angle (ΔDTA), are correlated (linear coefficient of correlation 0.72 and −0.77 for the dayside and nightside, respectively). The absolute value of the slopes s (=ΔCGL/ΔDTA) of the fitted lines were practically the same, with s(dayside) = -0.11 ± 0.01 and s(nightside) = $+0.10 \pm 0.02$. Thus the data in Figure 4 show that a 10° increase in the dipole tilt angle causes dayside auroral arcs to shift 1° equatorward, and nightside arcs to shift 1° poleward.

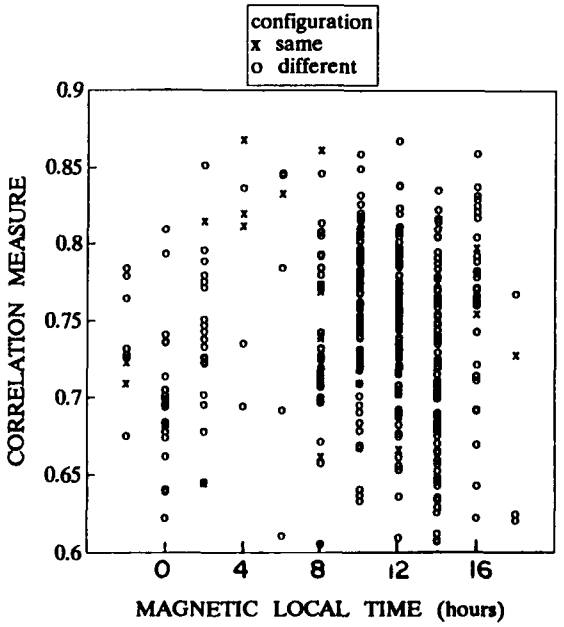

Fig. 3. Distribution of correlation measure values of quiet auroral images with MLT. Individual points are distinguished to represent pairs of images which belong to the same magnetospheric configuration (crosses) and to different magnetospheric configuration (circles). Each value represents a MLT sector 2 hours wide.

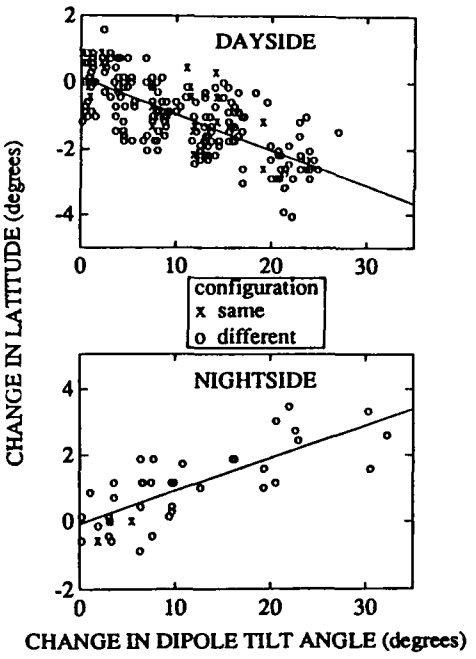

Fig. 4. Latitudinal shifts of auroral emissions related to changes in dipole tilt angle; 207 points contributed to the dayside analysis (top, 1200, 1400, and 1600 MLT) and 40 points to the nightside analysis (bottom, 2200, 0000, and 0200 MLT). The slopes of the straight lines, derived from a least chi-square fit to the data, are -0.11 ± 0.01 and $+0.10 \pm 0.02$ for the dayside and nightside, respectively.

DISCUSSION

The low value of the average correlation measure (0.74) prompts the immediate question of its significance. This question can only be answered by studying the uncertainties inherent in the image acquisition and processing leading to a given value of the correlation measure.

What is the lowest correlation measure that can be expected? We ran tests on 1000 pairs of synthetic images consisting of uniformly distributed noise. These images were produced by a random number generator to determine the count rate of every pixel. The average correlation measure for these 1000 pairs was 0.32 ± 0.02. What is the highest correlation measure that can be expected? In principle, the correlation measure of an image with itself is unity. Assuming one simultaneously acquired two images of the aurora from two identical instruments located at virtually the same point in space, would one get two identical ($r = 1$) images? The answer is obviously no. The reasons are errors in image pixel position and intensity that are inherent to the actual platforms, instruments, and reduction algorithms.

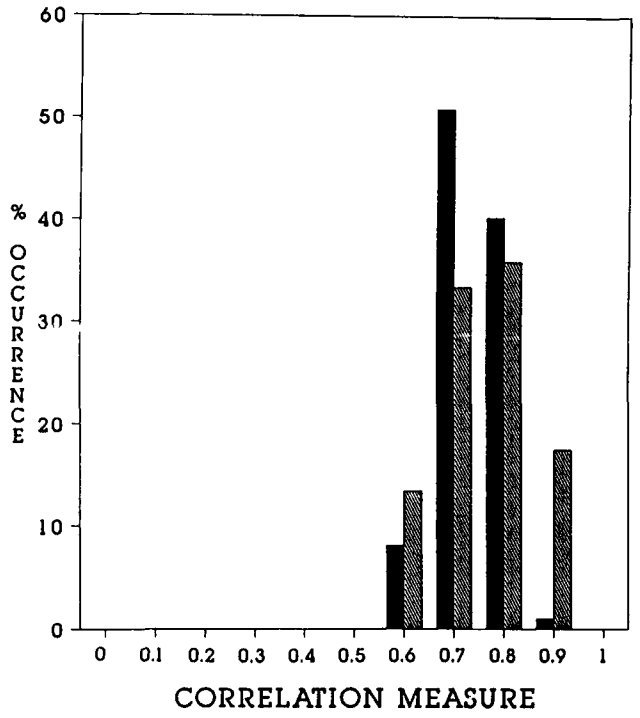

Fig. 5. A normalized distribution of correlation measures derived from an error analysis of randomized images (light shading). The purpose of this analysis was to determine the maximum expected value of the correlation measure. Dark shading denotes the normalized distribution of correlation measures of our 30 quiet state auroral images.

The question of the significance of the reported correlation measure values thus reduces to the following question: What is the correlation measure of an image with itself when uncertainties are considered? Two types of pixel uncertainty are considered: (1) position, use one standard deviation for a pixel position as 0.5° of corrected geomagnetic latitude; note that the expected average error in latitude (0.5°) corresponds to a 0.5°/cos (CGL) error in longitude, and (2) intensity, use a Poisson distribution with an average that equals the measured count rate of the input pixel. The 30 images that compose our data exhibit a dynamic range of 1–76 with an average of 7.2 counts.

The following algorithm was constructed to answer the question of the maximum expected value of the correlation measure. The algorithm is essentially an error simulator that correlates an image I with its counterpart I_u. I_u is produced from an input image I as follows:

1. Take a pixel from input image I with intensity i and corrected geomagnetic position (CGL, MLT).
2. Its new position in image I_u is chosen randomly from a two-dimensional normal distribution with average position (CGL, MLT) and a standard deviation (σ_{CGL}, σ_{MLT}) as specified above.
3. Its new intensity i_u in image I_u is chosen randomly from a Poisson distribution with average i.

To avoid gaps in I_u the above algorithm was implemented backward, i.e., the appropriate intensity and position in I were located for all the I_u pixels. Two input images, one covering dayside MLTs and one covering nightside MLTs, were chosen from the data. The MLT sectors covered were 1000, 1200, 1400, and 1600 MLT for the dayside image, and 0000, 0200, and 0400 MLT for the nightside image; 150 randomized images I_u were produced for each input image I. The 1050 calculations produced a range of correlation measures of 0.65–0.9 with an average of 0.76. Figure 5 shows a normalized number distribution of the correlation measure derived from this error analysis (light shading) relative to the distribution of 431 correlation measures of our 30 quiet state auroral images (dark shading). The two distributions are similar, with the error analysis distribution shifted to slightly higher values. The correlation measure of 0.74 relative to 0.76 should not be interpreted as an almost perfect correlation. We conclude that the auroral emissions observed are as repeatable (correlation measure 0.74) as can be expected considering the uncertainties in the observations. The expected uncertainties in pixel position and intensity limit the average correlation measure from identical images to 0.76.

It is interesting to note that pairs of auroral images, one of a quiet and the other of a disturbed magnetosphere, are still correlated, though at a lower level than pairs of auroral images both of the quiet magnetosphere. Fifteen images of the quiet magnetosphere (as defined above) were correlated with 15 images obtained at disturbed magnetospheric conditions ($Kp \geq 4$, no interplanetary data available). The average correlation measure of these quiet-active pairs was 0.6 ± 0.1.

The MLT distribution of correlation measures of the quiet-active pairs was markedly different from that of the quiet-quiet pairs. Figure 3 shows the MLT distribution of correlation measures for quiet-quiet pairs. Figure 6 shows the MLT distribution of correlation measures for quiet-active pairs. The correlation measure of quiet-quiet pairs is shifted to significantly higher values relative to the correlation measure of quiet-active pairs. The correlation measure of quiet-quiet pairs is independent of MLT and approximately constant at the 0.74 average. The correlation measure of quiet-active pairs is much lower in the nightside (0.3–0.5 at 0000 MLT) than in the dayside (0.5–0.8 at 1200 MLT). The fact that auroral emissions in active versus quiet magnetospheric conditions differ more around midnight than noon-

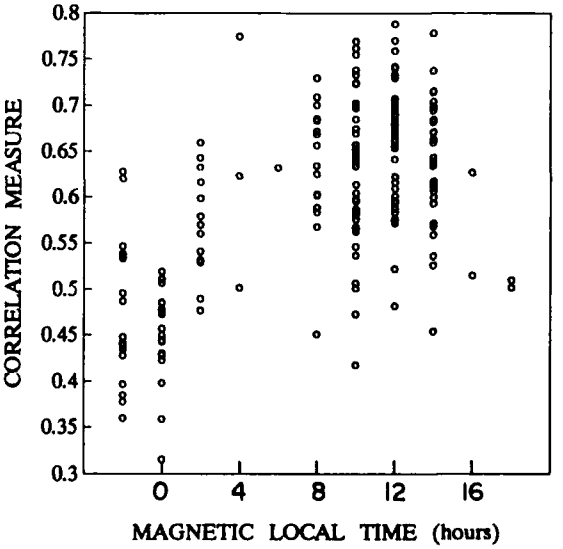

Fig. 6. Distribution of correlation measure values with MLT for quiet-active pairs. Each value represents a MLT sector 2 hours wide.

time is due to two facts. For a given detection threshold, the width of the nighttime auroral oval during substorms is 3–4 times greater than the corresponding width at quiet periods (low Kp). The width of the daytime auroral oval during substorms is only 2–3 times greater than the corresponding width at quiet periods. More importantly, spatial variability is greatest around midnight during substorms (auroral surges, the midnight bulge, etc.).

Our data indicate that the latitude of the continuous aurora depends on the dipole tilt angle. This dependence was studied at different local times. Figure 7 shows the slopes of least chi-square fit to ΔCGL/ΔDTA for eight MLT sectors: 0000, 0200, 0800, 1000, 1200, 1400, 1600, and 2200 (denoted by dots with bars). MLT sectors not shown in Figure 7 produced unreliable slopes due to their small number of correlation measures. The vertical error bars denote one standard deviation of the slopes. Horizontal bars depict the MLT range of the measurement (2 hours).

The MLT dependence of the latitudinal variation with dipole tilt angle follows a simple experimental model. The model describes the auroral oval as a circle with constant radius φ (for given IMF conditions). The center of the circle lies along the meridian AB, positioned ϕ_0 degrees from the dawn direction (0600 MLT), and located along AB φ_0 degrees antisunward of the magnetic pole. Figure 8 shows the change in position of the center of the auroral circle if the dipole tilt angle simply determines the location of the center of this circle along the meridian AB. A change in DTA, ΔDTA, thus corresponds to a shift of $\Delta\varphi_0$ degrees of the center of the auroral circle toward B. The change in CGL, ΔCGL, is marked $\Delta\varphi$ in Figure 8. The slope $s(\phi)$ is given by

$$s(\phi) = \frac{\Delta\text{CGL}}{\Delta\text{DTA}} = \frac{\Delta\varphi}{\Delta\varphi_0} = S\,\frac{(\varphi_0/\varphi) - \cos(\phi - \phi_0)}{1 - (\varphi_0/\varphi)\cos(\phi - \phi_0)} \qquad (4)$$

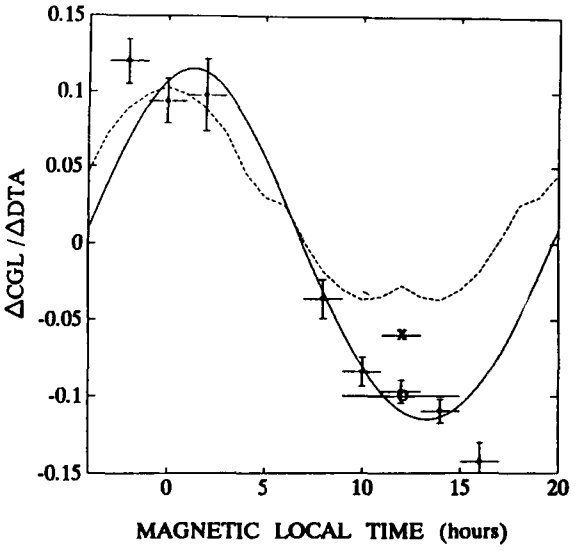

Fig. 7. Corrected geomagnetic latitudinal (CGL) shifts associated with changes in the dipole tilt angle (DTA) in the winter hemisphere. Dots with vertical and horizontal bars denote our data, showing the slopes of least chi-square fit to ΔCGL/ΔDTA for eight MLT sectors. Vertical error bars are one standard deviation of the slopes. Horizontal bars depict the MLT range of the measurement. A DTA dependence of the low-latitude boundary of soft particle precipitation associated with the cusp was found by *Burch* [1972], denoted by a circle, and *Newell and Meng* [1989], denoted by a cross. See text for description of curves.

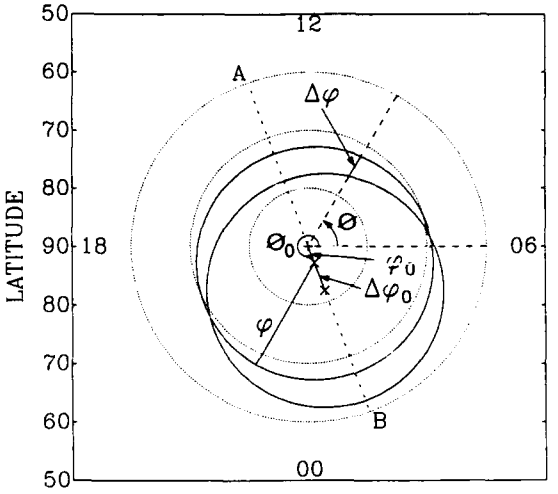

Fig. 8. A model of the effect of dipole tilt angle on the auroral circle. The dipole tilt angle determines the location of the center of the circle (φ_0) along the meridian AB with no change to its radius (φ). Here a change of $\Delta\varphi_0$ degrees in the location of the center of the auroral circle antisunward is related to a latitudinal shift of $\Delta\varphi$ degrees of the aurora as a function of MLT (parameterized by the angle ϕ). The predictions of this model agree with our data, as shown by Figure 7.

where S is the amplitude and $\phi = 2\pi(\text{MLT} - 0600)/24$.

A least chi-square fit of the three parameters of the model to the data shown in Figure 7 yielded $S = -0.115$, $\varphi_0/\varphi = 0.1$, and ϕ_0 corresponding to B = 0120 MLT with $\chi^2 = 8.6$. This fitted model is the solid curve of Figure 7. All the slopes $s(\phi)$ measured from our data lie within one standard deviation of the solid curve of Figure 7, with the exception of 1600 MLT, which lies within two standard deviations of it. Our data thus support the simplified view of a direct control of the dipole tilt angle over the center of the auroral circle with no change to its radius.

We now compare our results with other studies of dipole tilt angle effects on observables of the polar ionosphere. The center of the auroral circle in our fitted model is shifted dawnward of the midnight-noon meridian. This is in agreement with *Elphinstone et al.* [1990], who found IMF B_y positive to displace the northern hemisphere auroral distribution toward dawn. $\varphi_0/\varphi = 0.1$ of our fitted model is slightly below the expected value of 0.15–0.3. Previous studies showed that φ_0 = 3°–5° and φ = 15°–20° for our IMF conditions [*Holzworth and Meng*, 1975; *Meng et al.*, 1977].

The dashed curve of Figure 7 is the theoretical prediction of *Voigt* [1974] of the change in latitude with dipole tilt angle of the last closed field line boundary for the winter hemisphere (DTA = 90°–120°). The model matches the data reasonably well around midnight, as with other studies of the DTA effects on the auroral electrojet in the midnight polar cap [*de la Beaujardière et al.*, 1991; *Wu et al.*, 1991] (not shown in Figure 7). Our data show that as the DTA increases, nightside auroras shift poleward and dayside auroras shift equatorward. The crossover (no change in latitude with DTA) is approximately at 0700 MLT in the dawn side and at 1900 MLT in the dusk side (see Figures 7 and 8). This is in agreement with *Wu et al.* [1991], who placed the crossover 2–3 hours after dusk (no dawnside information available). There is also agreement on the dawnside with Voigt, whose Figure 4*b* shows the crossover points at 0700 and 1700 MLT.

The results of two studies of the daytime polar cusp are also shown in Figure 7. Both *Burch* [1972], denoted by a circle, and *Newell and Meng* [1989], denoted by a cross, found a DTA dependence of the low-latitude bound of soft particle precipitation associated with the cusp. Qualitatively, both our data and those of Burch and Newell and Meng support the prediction of the theoretical model suggested by Voigt in the daytime. Closed field lines, along with precipitating particles and auroral emissions, are traced to lower latitudes with increasing dipole tilt angles. Quantitatively, our data and those of Burch find the effect 2–3 times greater than either the model prediction or the data of Newell and Meng at noon.

The success of the simple model, presented by Figure 8, implies that the magnetosphere behaves almost like a rigid body in its response to changes in the dipole tilt angle. That is, very different parts of the magnetosphere move in unison with regard to the dipole tilt angle. The discrepancy between the magnitude of the phenomena between our results and those of *Newell and Meng* [1989] could be explained as follows. It is unclear whether our dayside data correspond to precipitation of plasma sheet origin or to precipitation of low-latitude boundary layer origin. It is clear that most of our emissions lie at the feet of closed field lines (see Figure 1) and are not related to cusp precipitation. Polar cusp precipitation, as in the case of Newell and Meng, is of magnetosheath origin and is traced down to the ionosphere along open field lines. Open field lines of magnetosheath origin may react differently than closed field lines with regard to dipole tilt angle changes. The majority of the low-energy electrons detected by *Burch* [1972] were also probably precipitating on closed field lines. Although Burch related his data to polar cusp precipitation, his low-energy electrostatic analyzer was sensitive to 0.7 keV electrons, an energy characteristic of auroral oval precipitation in that region at quiet times. Also, his low-latitude boundary of polar cusp precipitation (see his Figure 7; CGL = 75°–78° for DTA = 120°–90°) lies well within the boundary of the last closed field line and our auroral emissions (Figure 1). Several factors in the magnetospheric field model of *Voigt* [1974], such as the subsolar standoff distance and attributes of the neutral current sheet, could explain discrepancies between it and our data. However, it is not obvious from the Voigt model how changes of these parameters would effect the dipole tilt angle dependence of the last closed field line boundary.

CONCLUSIONS

Here the notion of a ground state magnetosphere and the dependence of the auroral oval size and position on the dipole tilt angle were investigated. A technique to discern latitudinal and longitudinal shifts of the aurora without resorting to boundary specification was offered. The correlation technique could also be employed on one dimensional data sets such as in-situ particle measurements.

Following *Kerns and Gussenhoven* [1990], the quiet magnetosphere was characterized by $B \leq 8$ nT, $|B_z| \leq 4$ nT, and $V < 500$ km s^{-1} using high temporal resolution IMP 8 data. All these conditions were required to be maintained at least 2 hours prior to image acquisition time. Analysis of far ultraviolet images of the aurora obtained by the Polar BEAR satellite at the above magnetospheric conditions indicate that the correlation measure of the auroral oval is independent of time or reconfigurations of the magnetosphere between images, and independent of magnetic local time. We find that the auroral oval has a definable quiescent state, one that is repeatable to a degree as high as can be expected considering inherent image uncertainties.

At periods of extreme magnetic and auroral quiescence the polar cap potential is at its minimum [*Heppner*, 1977]. The large-scale region 1 and 2 currents are usually absent, except in the polar cusp [*Hoffman et al.*, 1988]. *Akasofu* [1981] showed that the solar wind-magnetosphere energy coupling ϵ could be identified with the power of the solar wind-magnetosphere dynamo and that it correlates well with the total energy consumption rate of the magnetosphere. For our IMF conditions, the solar wind energy flux is at most 10^{18} erg s^{-1}. *Akasofu* [1981] showed that the development of magnetospheric substorms is a direct consequence of increasing ϵ above 10^{18} erg s^{-1}. Alternatively, the small B_z values ($|B_z| \leq 4$ nT) used in this study imply a slow reconnection rate. All these facts indicate that our auroral images not only represent the quiet auroral oval but are also a manifestation of the quiescent magnetosphere. Therefore we believe that the conclusions described here have global implications to the entire magnetosphere.

With regard to the question of dependence of auroral oval position and size on dipole tilt angle, our data indicate the following:

1. Changes in corrected geomagnetic latitude are related to changes in dipole tilt angle in the winter hemisphere for all MLT sectors.
2. A 10° increase in the dipole tilt angle causes a 1° decrease in the latitude of auroras at noon and a 1° increase in the latitude of auroras at midnight.
3. The magnetic local time distribution of the latitudinal shifts with dipole tilt angle support a simple model in which the dipole tilt angle determines the position of the center of the auroral circle along the meridian 1320–0120 MLT (for IMF B_y positive).
4. The radius of the auroral circle does not depend on the dipole tilt angle.

We have no way of switching off input power into the magnetosphere altogether. The solar wind never vanishes. The best chance of identifying the character of the quiet magnetosphere is to look for times with low solar wind velocities and interplanetary magnetic field magnitudes. At such times the output energy channels of the magnetosphere may be investigated to study its intrinsic structure and energetics. This paper investigated one such energy output, namely, far-ultraviolet auroral emissions. It was shown that this energy output is relatively constant in magnitude and structure, thereby supporting the notion of a ground state magnetosphere. Furthermore, it was shown that continuous auroral emissions that originate from precipitating particles on closed field lines depend in a simple manner on the dipole tilt angle. This phenomenon manifests itself as diurnal and seasonal changes in aurora position. Additional methods and other output energy channels of the magnetosphere must be investigated globally before we gain a clear understanding of the quiet magnetosphere.

Acknowledgments. This research was supported by the U.S. Air Force Office of Scientific Research under contract F49620-87-C-0091.

The Editor thanks the two referees for their assistance in evaluating this paper.

REFERENCES

Akasofu, S.-I., Energy coupling between the solar wind and the magnetosphere, *Space Sci. Rev.*, *28*, 121–190, 1981.

Burch, J. L., Precipitation of low-energy electrons at high latitudes: Effects of interplanetary magnetic field and dipole tilt angle, *J. Geophys. Res.*, *77*, 6696–6707, 1972.

Couzens, D. A., and J. A. King, Interplanetary medium data book, supplement 4, 1985–1988, *Rep. NSSDC 98-17*, Natl. Space Sci. Data Cent., World Data Cent. A for Rockets and Satell., Greenbelt, Md., Sept. 1989.

de la Beaujardière, O., D. Alcayde, J. Fontanari, and C. Leger, Seasonal dependence of high-latitude electric fields, *J. Geophys. Res.*, *96*, 5723–5735, 1991.

DelGreco, F. P., R. E. Huffman, J. C. Larrabee, R. W. Eastes, F. J. LeBlanc, and C.-I. Meng, Organizing and utilizing the imaging and spectral data from Polar BEAR, in Ultraviolet Technology II, *Proc. SPIE Int. Soc. Opt. Eng.*, *932*, 30–35, 1988.

Elphinstone, R. D., K. Jankowska, J. S. Murphree, and L. L. Cogger, The configuration of the auroral distribution for interplanetary magnetic field B_z northward, I, IMF B_x and B_y dependencies as observed by the Viking satellite, *J. Geophys. Res.*, *95*, 5791–5804, 1990.

Gussenhoven, M. S., Low-altitude convection, precipitation, and current patterns in the baseline magnetosphere, *Rev. Geophys.*, *26*, 792–808, 1988.

Gussenhoven, M. S., D. A. Hardy, and W. J. Burke, Comment on "Diurnal variation of the auroral oval size" by C.-I. Meng, *J. Geophys. Res.*, *85*, 2373–2374, 1980.

Hardy, D. A., M. S. Gussenhoven, and E. Holeman, A statistical model of auroral electron precipitation, *J. Geophys. Res.*, *90*, 4229–4248, 1985.

Heppner, J. P., Empirical models of high-latitude electric fields, *J. Geophys. Res.*, *82*, 1115–1125, 1977.

Hoffman, R. A., M. Sugiura, N. C. Maynard, R. M. Candey, J. D. Craven, and L. A. Frank, Electromagnetic patterns in the polar region during periods of extreme magnetic quiescence, *J. Geophys. Res.*, *93*, 14,515–14,541, 1988.

Holzworth, R. H., and C.-I. Meng, Mathematical representation of the auroral oval, *Geophys. Res. Lett.*, *2*, 377–380, 1975.

Kerns, K. J., and M. S. Gussenhoven, Solar wind conditions for a quiet magnetosphere, *J. Geophys. Res.*, *95*, 20,867–20,875, 1990.

Levine, M. D., *Vision in Man and Machine*, McGraw-Hill, New York, 1985.

Maehlum, B. N., Universal time control of the low-energy electron fluxes in the polar regions, *J. Geophys. Res.*, *73*, 3459–3468, 1968.

Meng, C.-I., Diurnal variation of the auroral oval size, *J. Geophys. Res.*, *84*, 5319–5324, 1979.

Meng, C.-I., R. H. Holzworth, and S.-I. Akasofu, Auroral circle: Delineating the poleward boundary of the quiet auroral belt, *J. Geophys. Res.*, *82*, 164–172, 1977.

Newell, P. T., and C.-J. Meng, Dipole tilt angle effects on the latitude of the cusp and cleft/low-latitude boundary layer, *J. Geophys. Res.*, *94*, 6949–6953, 1989.

Schenkel, F. W., B. S. Ogorzalek, R. R. Gardner, R. A. Hutchins, R. E. Huffman, and J. C. Larrabee, Simultaneous multi-spectral narrow band auroral imagery from space (1150 Å to 6300 Å), in Ultraviolet Technology, *Proc. SPIE Int. Soc. Opt. Eng.*, *687*, 90–103, 1986.

Stern, D. P., Parabolic harmonics in magnetospheric modeling: The main dipole and the ring current, *J. Geophys. Res.*, *90*, 10,851–10,863, 1985.

Voigt, G. H., Calculation of the shape and position of the last closed field line boundary and the coordinates of the magnetopause neutral points in a theoretical magnetospheric field model, *J. Geophys. Res.*, *40*, 213–228, 1974.

Wu, Q., T. J. Rosenberg, L. J. Lanzerotti, C. G. Maclennan, and A. Wolfe, Seasonal and diurnal variations of the latitude of the westward auroral electrojet in the nightside polar cap, *J. Geophys. Res.*, *96*, 1409–1419, 1991.

R. W. Eastes and R. E. Huffman, Phillips Laboratory, Geophysics Directorate, Hanscom AFB, MA 01731.

I. Glaser and M. Tur, Faculty of Engineering, Tel Aviv University, Ramat Aviv, Tel Aviv, Israel 69978.

I. Oznovich, ISAS, University of Saskatchewan, Saskatoon, Saskatchewan, Canada S7N 0W0.

(Received March 3, 1992;
revised July 16, 1992;
accepted August 10, 1992.)